Supplementary information

Supplementary Material and Methods

Polysome profile analysis

Synchronized worms were grown at 25 °C (N2 L3 and late L4, *let-7(n2853)* and *ain-2(tm1863);ain-1(RNAi)*) or at 20 °C (N2 L2 and *lin-4(e912)*) and on NGM (2%) plates seeded with *E. coli* OP50. L2 (~200'000), L3 (~50'000), or late L4 (~30'000) worms, staged by vulval and gonad development, were harvested and washed three times with cold M9 supplemented with 1 mM cycloheximide and once with Lysis Buffer (see composition below) without RNasin and PTE/DOC. Worms were pelleted and frozen in liquid N_2. Worms resuspended in 450µl of cold Lysis Buffer (20mM Tris pH 8.5, 140 mM KCl, 1.5 mM $MgCl_2$, 0.5 % Nonidet P40, 2% PTE (polyoxyethylene-10-tridecylether), 1% DOC (sodiumdeoxycholate monohydrate), 1mM DTT, 1mM cycloheximide, 0.4 U/µl RNasin) were crushed to a fine powder using mortar and pestle precooled with liquid N_2. As the powder thawed, lysates were collected and cleared by centrifugation (10 min. at 10'000 g, 4 °C).

Lysate absorbances at 260 nm were measured and equivalent amounts of material were loaded on sucrose gradients and centrifuged for 3 hours at 39'000 rpm, 4 °C, using a SW-40 rotor and an Optima™L-80 XP Ultracentrifuge (Beckman Coulter). Linear 15% to 60% (w/v) sucrose gradients were prepared from 15% (w/v) and 60% (w/v) sucrose solutions containing 20 mM Tris pH 8.5, 140 mM KCl, 1.5 mM $MgCl_2$, 1 mM DTT and 1 mM cycloheximide using a Gradient Master (Biocomp).

Gradient fractionation was performed using a Tris Pump (Teledyn ISCO), a Gradient Fractionator (BR-184-X, Brandel), and a fraction collector (FC-203B, Gilson). Absorbance profiles were recorded at 254 nm with an Econo UV monitor EM-1 (Biorad) coupled to a data acquisition device (DI-158U, DATAQ Instruments) using the WinDaq Serial Acquisition software (version 3.17). Gradients were fractionated in 12 fractions of equal volume. RNA from lysates and from each fraction was extracted with TRIzol (Invitrogen), according to the manufacturer's recommendations. RNA aliquots were quality controlled on ethidium bromide stained agarose gels prior to RT-qPCR analysis. For EDTA treatment, cycloheximide was omitted in M9, lysis buffer and sucrose solution and 10 mM EDTA was added to the lysis buffer and sucrose solutions. Incubation of extracts with puromycin (5mM for 20 min. at 37 °C) led to collapse of the polysomes, confirming their translational competence. Unexpectedly, all mRNAs, including those not known to be regulated by miRNAs, shifted towards dense sucrose gradients under these conditions, suggesting that the ribosome-free RNAs aggregated.

β-galactosidase assay

CT5a, HW211 and HW390 animals were grown on DH5α bacteria that lack β-galactosidase activity. Two animals of the desired stage were transferred into 1.5 µl BGA buffer (50 mM potassium phosphate, pH 7.2, 1 mM $MgCl_2$) and fixed and permeabilized by addition of 15 µl ice-cold acetone. Animals were resuspended in 8 µl of CPRG staining solution (1.5 mM CPRG [chlorophenolred-ß-D-galactopyranoside] in BGA buffer) and incubated for 1 h to 24 h at 37 °C. Aliquots of 2 µl were measured on a Nanodrop spectrophotometer at $\lambda = 575$ nm and corrected for absorption at $\lambda = 700$ nm. Enzyme activities remained stable over the whole period as determined by constant changes in extinction per hour and worm measured

for different time points. No difference in β-galactosidase activity was seen for transgenic animals grown at either 20 °C or 25 °C; animals lacking *lacZ* transgenes did not exhibit any β-galactosidase activity. Correct stages were confirmed by subsequent DAPI staining of the animals used for the assay and microscopic analysis of the gonad.

Classical PCR and quantification

Classical RT-PCRs were performed on cDNA prepared as mentioned in the experimental procedures section of the main text. PCRs were performed using Taq DNA polymerase (Qiagen) according to the manufacturer's recommendations. *lin-14*, *lin-41*, and *tbb-2* mRNA level were determined using same set of primers as for RT-qPCR reactions (qPCR lin-14 F2/R2, qPCR lin-41 F/R, qPCR tbb-1 F1/R1, respectively). PCR products were resolved on SyberSafe (Invitrogen) stained agarose gels. Quantification of the PCR products was performed by densitometry analysis of agarose gel pictures using the ImageJ software (http://rsbweb.nih.gov/ij/index.html).

Oligonucleotide sequences

Oligonucleotides used in the present study. The qPCR CT5a F1 and R1 primers were used to detect the *lacZ::lin-41* reporter mRNAs. The forward primer is complementary to the lacZ sequence and the reverse primer to the lin-41 3'UTR.

Name	5' to 3' sequence
qPCR act-1 F1	GTTGCCCAGAGGCTATGTTC
qPCR act-1 R1	CAAGAGCGGTGATTTCCTTC
qPCR ama-1 F1	GGATCGAAGGGATCGAAGA
qPCR ama-1 R1	TGGAAGAAGAATTCCGATGG
qPCR daf-12 F2	GATCCTCCGATGAACGAAAA
qPCR daf-12 R2	CTCTTCGGCTTCACCAGAAC
qPCR daf-12 F3	TTATATCCCGGCCACTCTCA
qPCR daf-12 R3	TGGAACACCAGGTAACGACA
qPCR lin-41 F1	GGATTGTTCGACACCAACG
qPCR lin-41 R1	ACCATGATGTCAAACTGCTGTC
qPCR CT5a F1	CGGTCGCTACCATTACCAAC
qPCR CT5a R1	CTGGAATGTGTGTGCTTTGC
qPCR pha-4 F1	CATGCAAGGAGGAGGAATTT
qPCR pha-4 R1	TCGTGAGTTCTTGGCCTTG
qPCR vit-1 F1	GAGGTTCGCTTTGACGGATA
qPCR vit-1 R1	GGCTTCACATTCCTCGTTCT
qPCR ugt-63 F1	AAAGACCCCCTGGATTGAAG
qPCR ugt-63 R1	TCTCTTTGATGAGCCAAGCA
qPCR tbb-2 F1	CAAATTCTGGGAGGTCATCTC
qPCR tbb-2 R1	CATACTTTCCGTTGTTGGCT
qPCR eft-2 F1	TGTGTTTCCGGAGTGTGTGT
qPCR eft-2 R1	CCATCGTCGTCTCCGTAAGT
qPCR hbl-1 F1	ACTGCACATATGCCACCAAA
qPCR hbl-1 R1	TGATGTAACCGGCTCAACTG
qPCR cog-1 F1	TCCAGCACTCAATGCAACTC
qPCR cog-1 R1	TTTTGTACGACGGTTTTGGA
qPCR lin-14 F1	TGCAAATCTTCCAATCAAAGG
qPCR lin-14 R1	TTCTGCCTGAGCCTCTTCTC
qPCR lin-14 F2	GGATTCAATGCGACAGGATT
qPCR lin-14 R2	CGATGCTGGTTTCAATGATG
qPCR lin-28 F1	ATTCAAGAGCGATCGAATGG
qPCR lin-28 R1	CACACTTTTGCATCGGTTTTT

NB lin-41 F1	CAAGACTCCTTTCGGTGCTC
NB lin-41 R1	CTGCACGGCTCATCAAAGTA
NB act-1 F1	GTTGCCCAGAGGCTATGTTC
NB act-1 R1	CAAGAGCGGTGATTTCCTTC

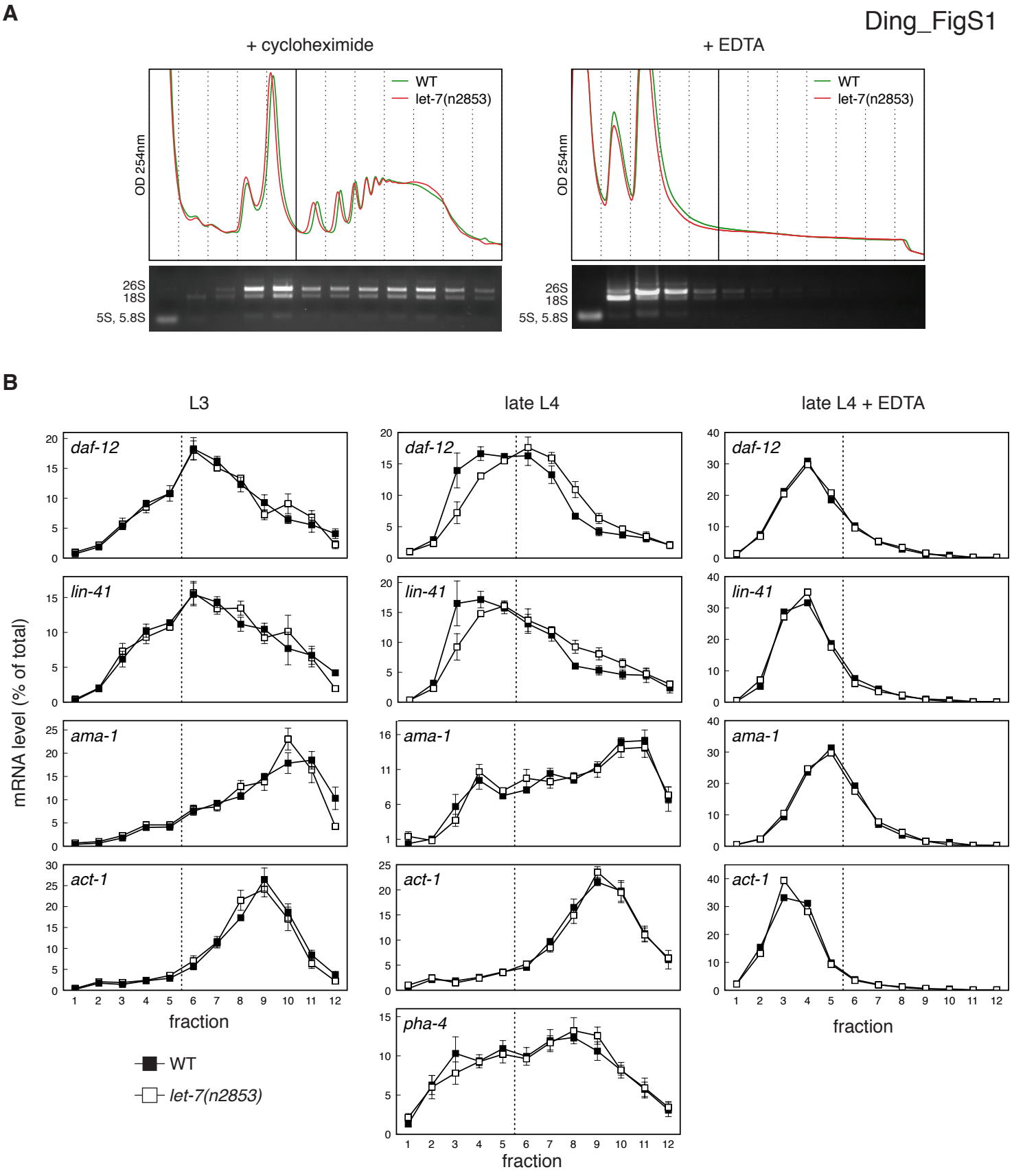

Figure S1: Polysome profile distribution of endogenous *let-7* target mRNAs.
(**A**) Typical polysome profiles from synchronized late L4 wild-type and *let-7(n2853)* animals in the presence of cycloheximide or EDTA, respectively. The solid line represents the separation between the (sub)monosomal and polysomal fractions. Lower panels are ethidium bromide stained agarose gels of RNA extracted from polysome profile fractions. The 26S, 18S, 5.8S and 5S rRNAs are visible. As indicated by absorbance profiles at 254 nm and rRNA distributions across fractions, cycloheximide treatment preserves polysome integrity, whereas EDTA treatment induces ribosome dissociation into 40S and 60S ribosomal subunits. Note that the absorbance profiles are those also shown in Fig. 1 (**B**) Distribution of the *let-7* targets *daf-12* and *lin-41* and of the control genes *ama-1* and *act-1* across polysome profiles from synchronized wild-type and *let-7(n2853)* L3 animals treated with cycloheximide, late L4 animals treated with cycloheximide, and late L4 animals treated with EDTA. *pha-4* distribution is shown for synchronized wild-type and *let-7(n2853)* late L4 animals only. The dotted line represents the separation between the (sub)monosomal and polysomal fractions. Panel B, except EDTA treatment, shows averages of at least three biological replicates. EDTA treatment was performed in duplicate, one representative experiment is shown. Error bars are SEM. *daf-12* and *act-1* data are as in Fig. 1 and included for comparison.

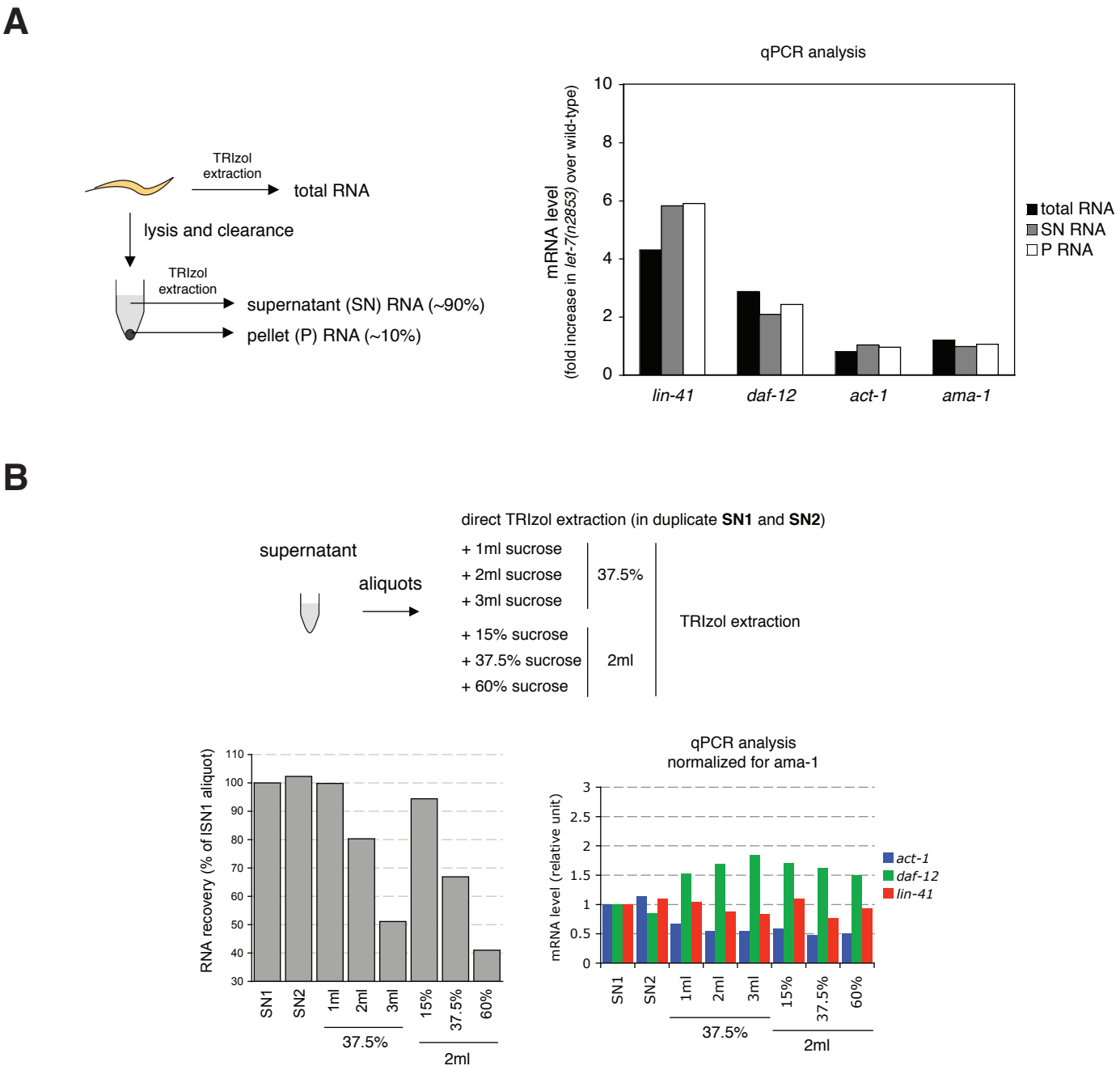

Figure S2: Analysis of RNA recovery from *C. elegans* lysate and polysome profile sucrose fractions.
(**A**) Synchronized L4 wild-type and *let-7(n2853)* animals were either resuspended in TRIzol or in polysome profile lysis buffer and crushed in mortar and pestle precooled with liquid nitrogen. RNA from worms resuspended in TRIzol was purified according to manufacturer's instruction. Lysate of worms resuspended in lysis buffer was cleared by centrifugation (see material and methods). RNA from the supernatant and the pellet was extracted using TRIzol. Approximately 90% of the RNA that can be recovered from direct TRIzol extraction is found in the supernatant for both wild-type and *let-7(n2853)* animals as determined by spectrophotometric analysis. Equal amounts of each RNA samples were reverse transcribed using random hexamer and relative abundance of the two *let-7* tragets *daf-12* and *lin-41* and of the two control genes *act-1* and *ama-1* was determined by qPCR. No enrichment of any mRNA can be detected in the supernatant or pellet samples as compared to total RNA. (**B**) Aliquots from one whole worm lysate (corresponding to SN in (A)) were either used for direct RNA extraction or mixed with sucrose solutions to obtain the indicated volume and concentration before RNA extraction. Although the amount of RNA recovered form lysates decreases when mixed with higer volume or higher concentration of sucrose solution, the relative abundance of *let-7* targets (*daf-12* and *lin-41*) and of *act-1* is only modestly (less than two-fold) affected as determined by random hexamer-primed RT-qPCR. Nevertheless, the sucrose concentration of polysome profile fractions was adjusted to 30% (w/v) before RNA purification in order to avoid underestimating the amount of RNA present in the deep part of the gradients.

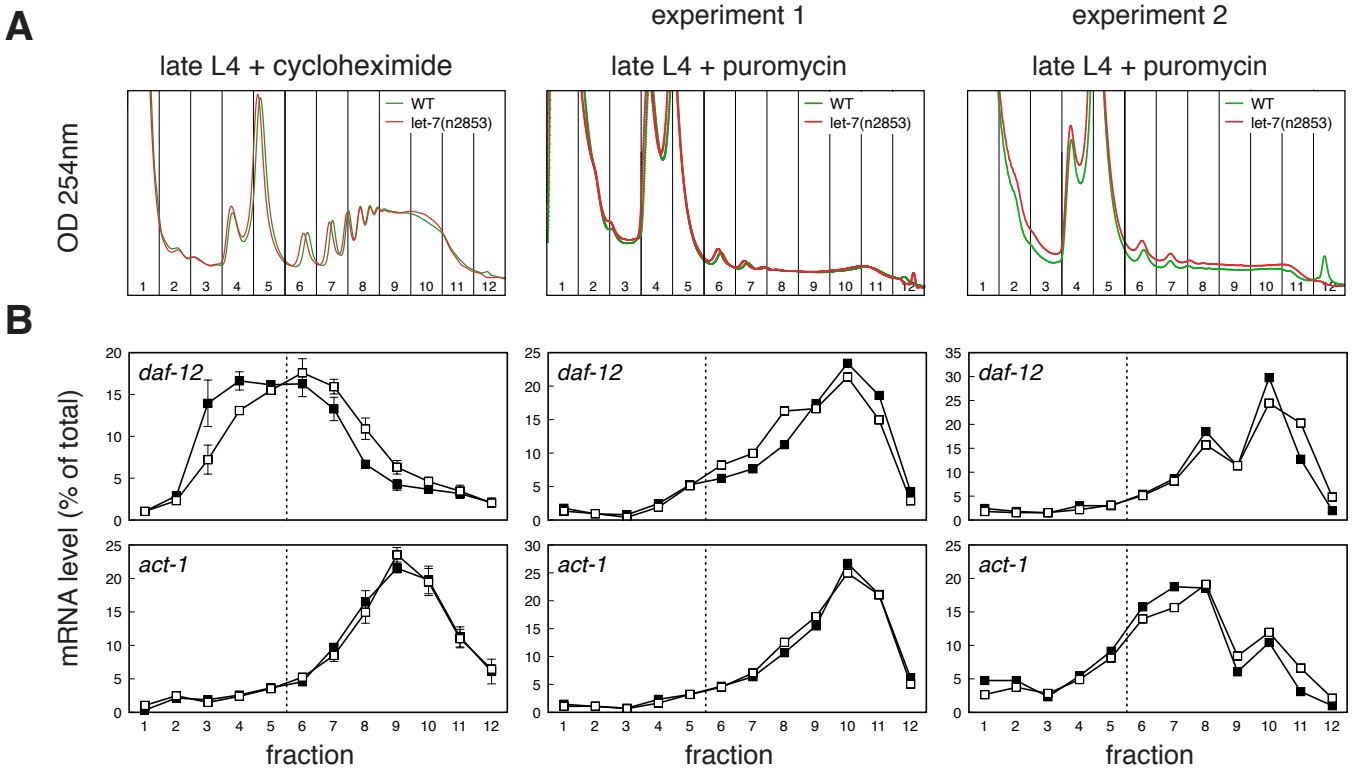

Figure S3: Puromycin treatment of *C. elegans* extract induces polysome dissociation.
(**A**) Typical polysome profiles from synchronized late L4 wild-type and *let-7(n2853)* animals in the presence of cycloheximide or puromycin. The solid line represents the separation between the (sub)monosomal and polysomal fractions. As indicated by absorbance profiles at 254 nm cycloheximide treatment preserves polysome integrity, whereas puromycin treatment induces polysome dissociation. Note that the absorbance profiles with cycloheximide are those also shown in Fig. 1 and S1. (**B**) Distribution of the *let-7* target *daf-12* and of the control gene *act-1* across polysome profiles from synchronized wild-type and *let-7(n2853)* late L4 animals treated with cycloheximide or puromycin. The dotted line represents the separation between the (sub)monosomal and polysomal fractions. Puromycin treatment collapses the elongation competent polysomes and no difference can be observed for *daf-12* distribution between wild-type and *let-7(n2853)* animals, indicating that the differential distribution observed in cycloheximide treated samples is due to differences in ribosome load on *daf-12* mRNAs. Surprisingly, all mRNAs, including mRNAs not targeted by miRNA, shift to denser fractions of the gradients under these conditions, suggesting that the ribosome-free mRNAs aggregate. For cycloheximide treatment, the averages of four biological replicates is shown and error bar are SEM, data are as in Fig. 1 and S1 and included for comparison.

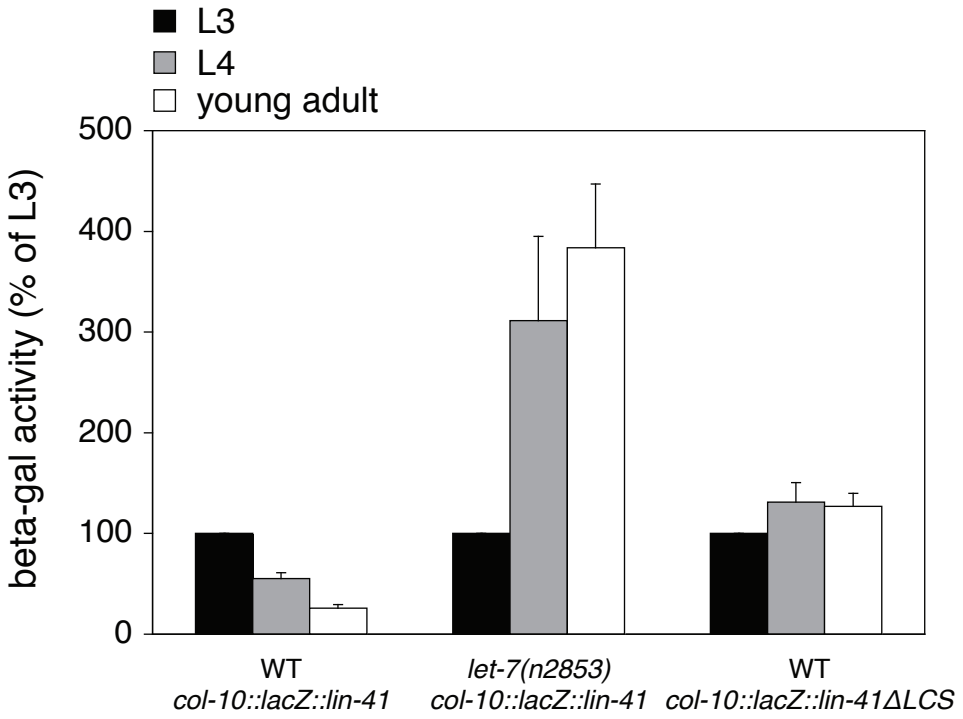

Figure S4: *lin-41* 3'UTR confers *let-7* mediated regulation
Quantitative measurement of the β-galactosidase (β-gal) activity in the different col-10::lacZ::lin-41 reporter strains shows that protein production is increased for the transgene lacking the *lin-41* LCSs or in *let-7* mutant worms, resulting in a respective five- and fifteen-fold increase in young adult compared to the activity in WT worms expressing a construct containing a full length *lin-41* 3'UTR. The lower level of β-Gal activity seen with the ΔLCS construct may indicate that other regulatory sites are still present in this 3'UTR. Averages of three biological replicates are shown, error bars are SEM.

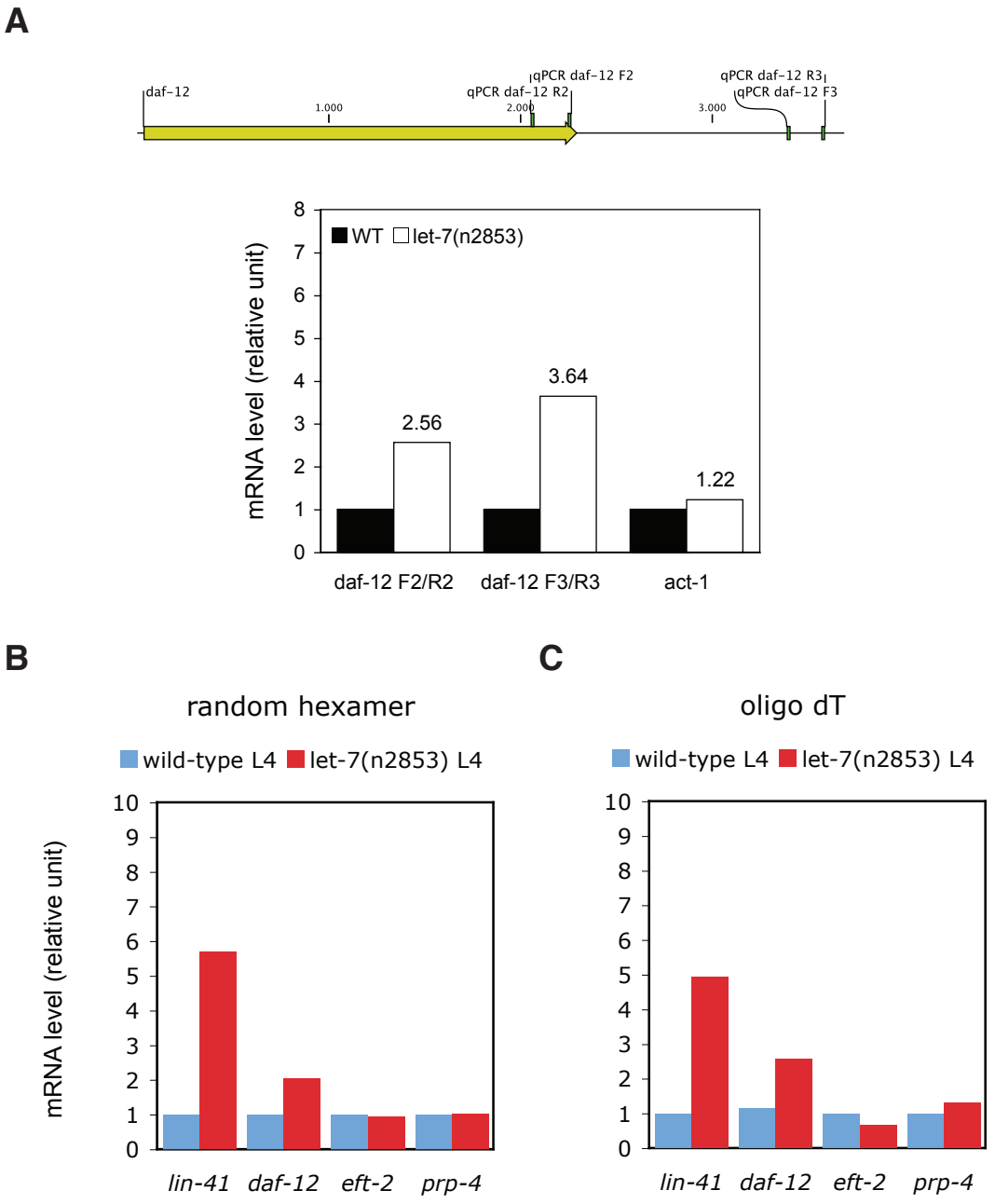

Figure S5 RT-qPCR validation

(**A**) *daf-12* total mRNA levels of synchronized late L4 wild-type and *let-7(n2853)* worms were determined by RT-qPCR using two distant pairs of primers: "qPCR daf-12 F2/R2" which amplify a fragment in the coding region and "qPCR daf-12 F3/R3" which amplify a fragment in the 3'UTR. The similarity of the results obtained with both primer pairs indicates that full length mRNA only is quantified.

(**B-C**) Reverse transcription reactions were performed on aliquots of the same total RNA extracted from wild-type and *let-7(n2853)* late L4 synchronized worms. The relative abundance, as determined by qPCR, of two *let-7* targets (*lin-41* and *daf-12*) and of two control genes (*eft-2* and *prp-4*) was found to be similar for reactions using random hexamer (**B**) and oligo dT primers (**C**). This indicates that mRNA levels determined using random hexamer represent full length mRNAs and that any effect miRNAs might have on polyA tail lengths of their targets does not prevent efficient oligo dT-primed reverse transcription.

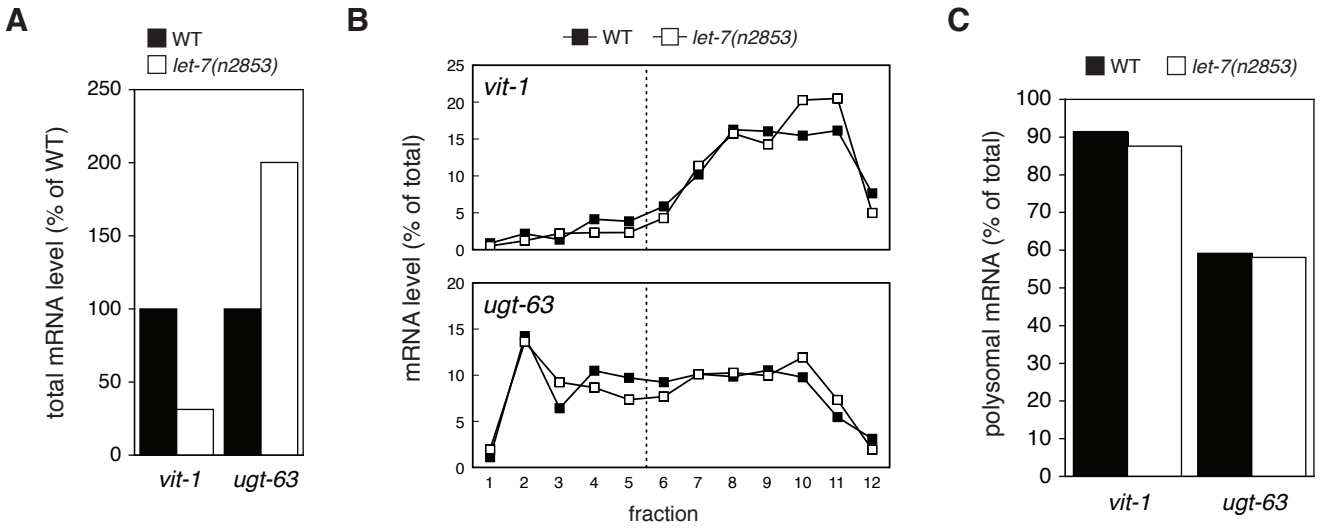

Figure S6: Changes in total mRNA levels do not influence translation initiation.
Although *vit-1* and *ugt-63* are differentially expressed in wild-type and *let-7(n2853)* animals, these genes are equally efficiently translated in both strains. (**A**) Analysis of *vit-1* and *ugt-63* total mRNA levels in synchronized late L4 wild-type and *let-7(n2853)* animals by RT-qPCR. (**B**) Distribution of *vit-1* and *ugt-63* mRNAs across polysome profiles from synchronized late L4 wild-type and *let-7(n2853)* animals. (**C**) Polysomal *vit-1* and *ugt-63* mRNA in late L4 wild-type and *let-7(n2853)* animals as percentage of the total. Averages of two biological replicates are shown for each panel**.**

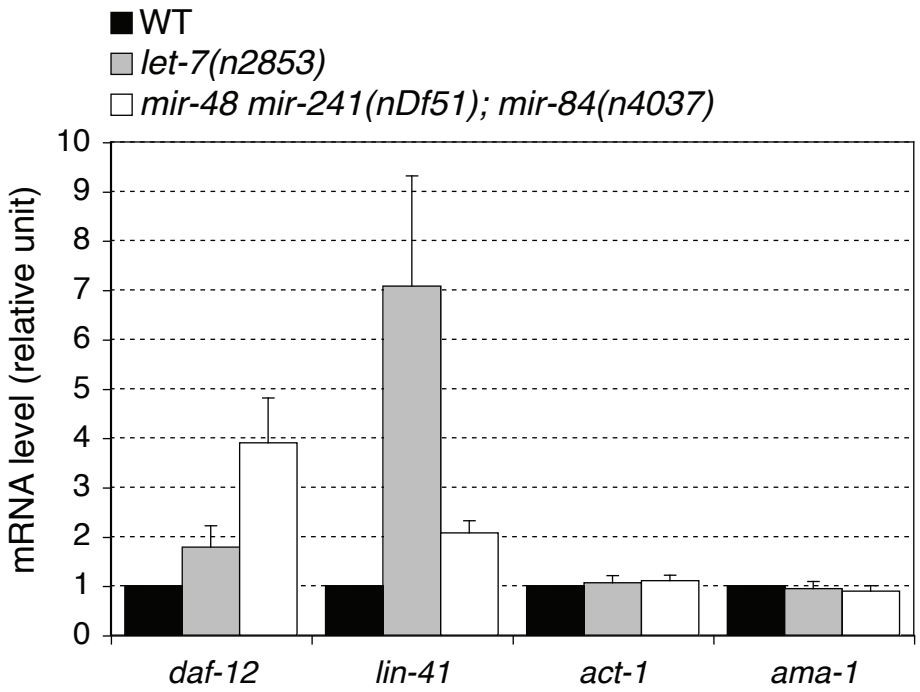

Fig. S7 Regulation of *let-7* targets by *let-7* sister miRNAs.
Analysis of the *let-7* target *daf-12* and *lin-41* and of control genes *act-1* and *ama-1* total mRNA levels in synchronized late L4 wild-type, *let-7(n2853)* and *miR-48 miR-241(nDf51); miR-84(n4037)* animals by RT-qPCR. Both *let-7* targets are also regulated by *miR-48*, *miR-84*, and *miR-241* although to different extents, which may be due to different temporal and spatial co-expression pattern with *daf-12* and *lin-41* (n=3, error bars are SEM).

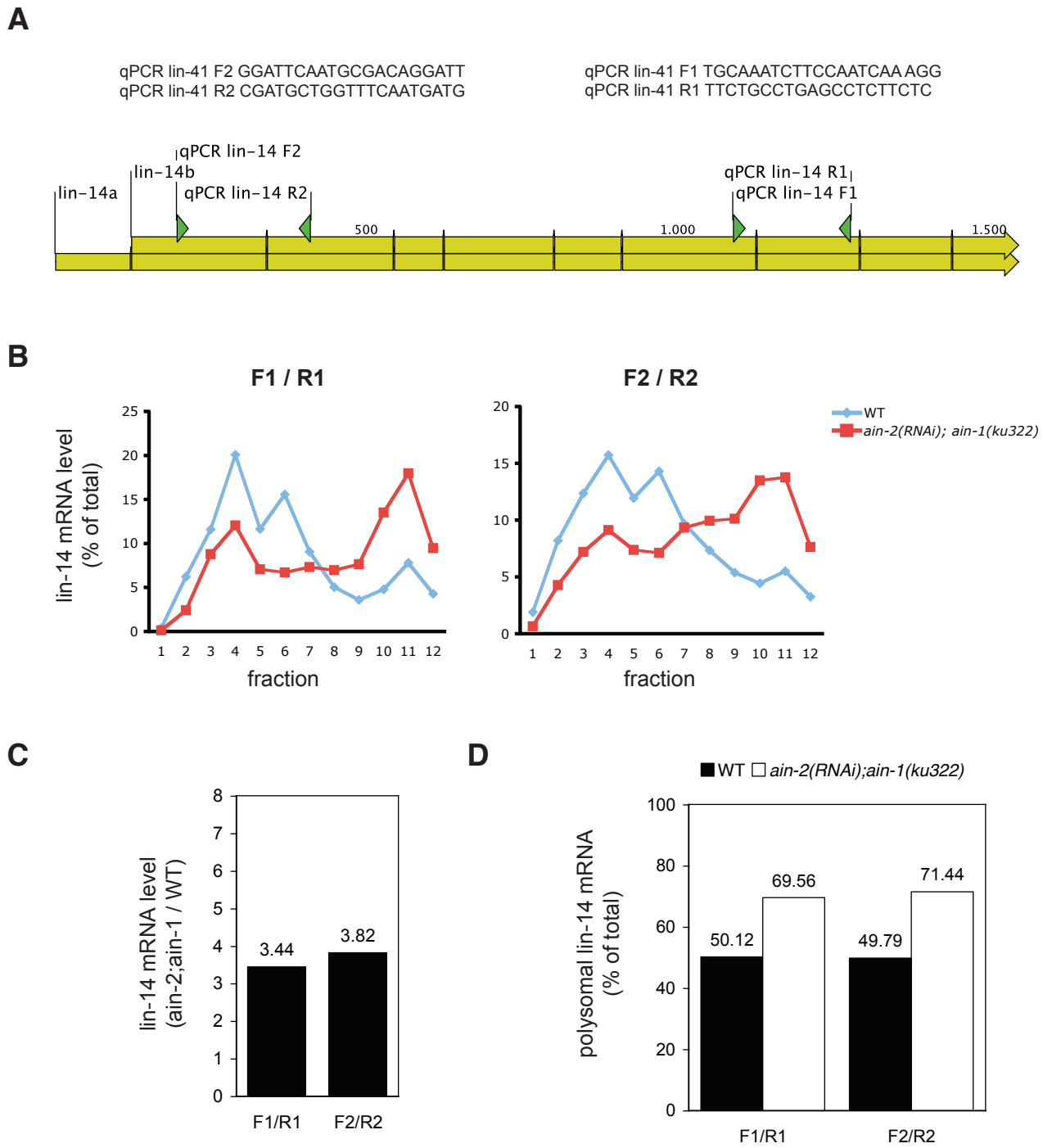

Figure S8 Comparison of two *lin-14* primer pairs

lin-14 total mRNA level and distribution across polysome profile of synchronized L4 wild-type and *ain-2(RNAi);ain-1(ku322)* animals were tested by RT-qPCR using two different pairs of primers amplifying distant regions from the same cDNA preparation. The similarity between the results obtained with both primer pairs indicates that full length mRNAs and not stabilized degradation products are quantified. (**A**) Schematic representation of the region amplified by RT-qPCR. (**B**) Polysome profile distribution. (**C**) Total mRNA level. (**D**) Percentage of mRNA in the polysomal fractions.

Ding_FigS9

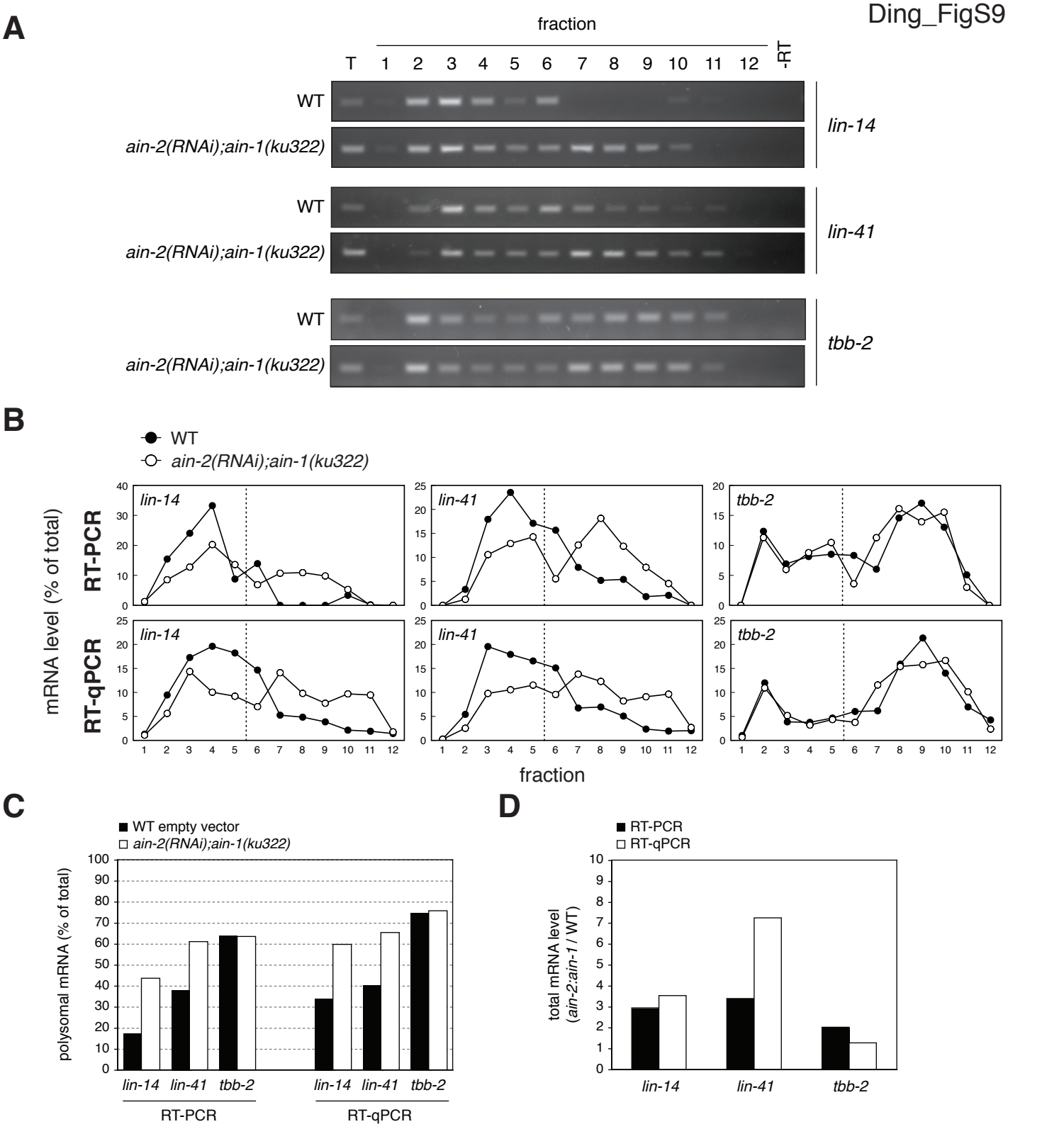

Fig. S9 Comparison between RT-qPCR and RT-PCR analyses.
(**A**) cDNA of total RNA and of RNA from polysome profile of synchronized L4 wild-type and *ain-2(RNAi);ain-1(ku322)* animals was used for semi-quantitative classical PCR. Aliquots of PCR reactions were analyzed on SybrSafe stained agarose gel. Distribution of both miRNA targets *lin-14* and *lin-41*, but not the *tbb-2* control mRNA, is shifted toward the polysomal fractions in *ain-2(RNAi);ain-1(ku322)* animals as compared to wild-type. Note that for each mRNA, wild-type and *ain-2(RNAi);ain-1(ku322)* samples were loaded on the same gel and photographed under identical conditions but are represented as separate pannels for better comparison. T, total RNA, -RT, negative control reaction lacking the reverse transcriptase using RNA from fraction 5. (**B**) Quantification of pictures shown in panel A was performed by densitometry analysis and is reported as percentage of the total. Note that values are corrected for total amount of RNA recovered from each fractions. Results from RT-qPCR analysis are shown for comparison. (**C**) Polysomal fraction of *lin-14*, *lin-41* and *tbb-2* mRNAs in synchronized L4 wild-type and *ain-2(RNAi);ain-1(ku322)* animals as percentage of the total determined by RT-PCR and RT-qPCR (**D**) Total levels of *lin-14*, *lin-41* and *tbb-2* mRNAs in synchronized L4 wild-type and *ain-2(RNAi);ain-1(ku322)* animals as fold increase in *ain-2(RNAi);ain-1(ku322)* animals compared to wild-type determined by RT-PCR and RT-qPCR. The overall results obtained by RT-PCR are similar to the ones obtained by RT-qPCR, confirming the validity of the latter method.